Secrecy Performance for Hybrid RF/VLC DF Relaying Systems

Jiaoli Liu
Shandong Key Laboratory of Optical Communication Science and Technology / Liaocheng University, Liaocheng, China
liujiaoli199671@163.com

Jinyuan Wang
Key Laboratory of Broadband Wireless Communication and Sensor Network Technology / Nanjing University of Posts and Telecommunications, Nanjing, China
jywang@njupt.edu.cn

Qinglin Wang*
Shandong Key Laboratory of Optical Communication Science and Technology / Liaocheng University, Liaocheng, China
wangqinglin@lcu.edu.cn

ABSTRACT

This letter studies the security performance of hybrid radio frequency (RF) and visible light communication (VLC) system. In this hybrid system, the source node (i.e., Alice) transmits information to the relay node via the outdoor RF link. Nakagami-m fading and path loss are considered for the RF link. The relay using the decode-and-forward (DF) relaying scheme. A legitimate receiver (Bob) arranged on the floor receives the optical signal. An eavesdropper (Eve) deployed in VLC link wiretaps the confidential information. In this paper, secrecy outage probability (SOP) is used to assess the performance of the system. We derive the closed expression of the lower bound of SOP when VLC link is wiretapped. Numerical results to validate the accuracy of our derivation.

CCS CONCEPTS

• **Security and privacy**; • **Network security**;

KEYWORDS

Visible light communications, radio frequency communications, secrecy outage probability

ACM Reference Format:
Jiaoli Liu, Jinyuan Wang, and Qinglin Wang*. 2021. Secrecy Performance for Hybrid RF/VLC DF Relaying Systems. In *International Conference on Frontiers of Electronics, Information and Computation Technologies (ICFEICT 2021), May 21–23, 2021, Changsha, China.* ACM, New York, NY, USA, 5 pages. https://doi.org/10.1145/3474198.3478226

1 INTRODUCTION

In recent years, visible light communication (VLC) technology has become a very promising technology. Compared to a radio frequency (RF) communication for VLC has many advantages: anti-electromagnetic interference, high bandwidth, large capacity, and low power consumption. In addition, VLC is not harmful to health [1]. VLC attracts a wide range of applications. Although VLC technology has many advantages and is widely used. However, its use is disturbed by shortcomings, such as the transmission performance of VLC is greatly reduced in the environment without line-of-sight (LoS) and VLC has a small coverage area [2]. Therefore, in the absence of LoS, the performance of the VLC system will be greatly reduced. Moreover, the light emitted by a light-emitting diode (LED) in VLC is easily blocked by obstacles [3}–8]. Therefore, a hybrid RF/VLC system was mentioned to solve the above problems. This kind of hybrid system can not only improve user speed and mobility, but also reduce interference and power consumption while increasing the capacity of the entire system [9].

Another critical problem in wireless communication is the confidentiality of information as wireless systems are vulnerable to security threats due to their inherent nature [10]. So far, the security of wireless communication has been provided by various encryption/decryption methods, which are performed at the upper layer of the protocol stack [11]. Physical layer security (PLS) is a supplementary or even alternative technology, which uses the randomness and time-varying of the wireless system to solve the security problem of the physical layer [12]. In [7], the PLS characteristics of hybrid RF/VLC systems and the problem of minimizing power consumption are studied. In [13], Based on the known and known channel state information (CSI) conditions, the PLS characteristics of the indoor RF/VLC system were analyzed. investigated the PLS transmission of VLC with simultaneous light wave information and power transfer. [14].

As far as the author knows, there are few literatures about the PLS performance analysis of the hybrid RF/VLC dual-hop system based on DF relay. Therefore, in this letter, we analyze the SOP of the proposed hybrid system. Among them, the first hop of the hybrid system is the RF link. For general considerations, we assume that the channel characteristics of the RF link can be characterized by path loss and Nakagami-m fading. Besides, in order to meet the actual illumination requirements of the VLC system, we assume that the optical signal is a non-negative signal and the average optical intensity signal is a fixed value. Therefore, Shannon's capacity is not suitable for analyzing the channel capacity of the VLC link. Based on the above considerations, it is necessary to analyze the PLS performance of the hybrid RF/VLC dual-hop relaying systems.

2 SYSTEM MODEL

As depicted in Fig. 1, a dual-hop hybrid RF/VLC network considered, which includes an outdoor RF link and an indoor VLC link. The hybrid network is composed of a source node (Alice): a relay node, an eavesdropper (Eve) and a legitimate receiver (Bob). The relay node includes an outdoor component and an indoor component, which are connected by using a wired medium. In this paper, we

ICFEICT 2021, May 21–23, 2021, Changsha, China

ACM ISBN 978-1-4503-9014-9/21/05…$15.00
https://doi.org/10.1145/3474198.3478226

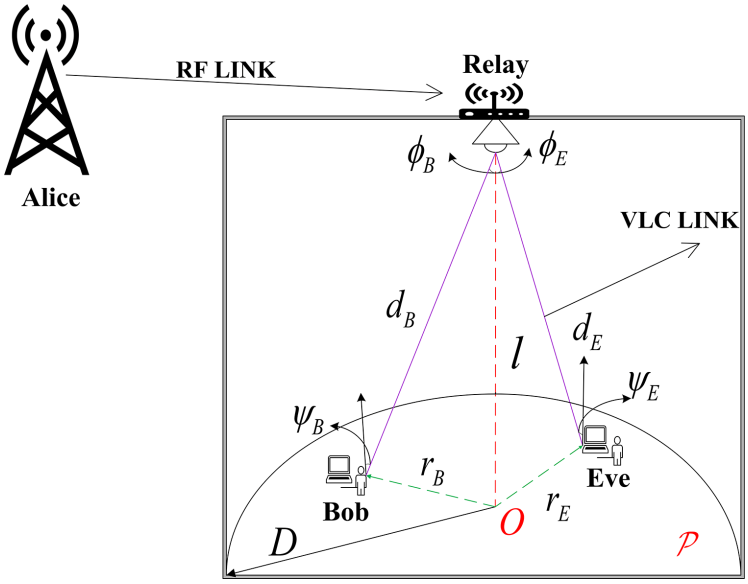

Figure 1: An RF/VLC hybrid communication network.

assume that outdoor component receives and recovers information by using the DF relay scheme, and then transmits it to the indoor component. The indoor component converts the received electrical signal to an optical signal by using an LED. There is no direct communication between Alice and Bob, information must be transmitted through the relay node. Alice sends confidential signal x to the outdoor component of the relay over the RF channel. The indoor component of the relay forwards the optical signal X to Bob through the indoor VLC channel. Both Bob and Eve deploy photodiodes to receive information and perform photoelectric conversion. When Alice transmits to Bob, Eve attempts to intercept the secret information.

2.1 RF Link

The signal received by the relay node in the RF link can be written as

$$y = \sqrt{P_s} h_{\mathrm{SR}} x + n_{\mathrm{R}} \tag{1}$$

where P_s represents the transmission power at Alice, h_{SR}denotes the channel gain of the RF link, and n_{R} is additive white Gaussian noise (AWGN) with mean zero and variance N_0.

The instantaneous signal-to-noise ratio (SNR) $\gamma_{\mathrm{SR}}$of relay node is

$$\gamma_{\mathrm{SR}} = P_s |h_{\mathrm{SR}}|^2 \Big/ N_0 \tag{2}$$

In the RF link, $|h_{\mathrm{SR}}|^2$in (2) can be expressed as

$$|h_{\mathrm{SR}}|^2 = |g_{\mathrm{R}}|^2 G_{\mathrm{R}} \tag{3}$$

where g_{R} and G_{R} represent fading and path loss respectively, and these two terms are independent of each other. The envelope of $g_{\mathrm{R}}$is assumed to follow the Nakagami-m distribution. Therefore, according to ref. [15] we can know that the probability density function (PDF) of $|g_{\mathrm{R}}|^2$ is

$$f_{|g_{\mathrm{R}}|^2}(x) = \frac{x^{m_{\mathrm{R}}-1}}{\Gamma(m_{\mathrm{R}})} {m_{\mathrm{R}}}^{m_{\mathrm{R}}} \exp(-m_{\mathrm{R}} x), x \geq 0 \tag{4}$$

where m_{R} represents the fading factor, Ω represents the average power of the signal, $\Gamma(m_{\mathrm{R}}) = \int_0^{+\infty} x^{m_{\mathrm{R}}-1} e^{-x} dx$ represents the Gamma function.

Furthermore, G_{R}in (3) can be modeled as [15]

$$G_{\mathrm{R}} = \left(\frac{d_0}{d_1}\right)^{\lambda} \tag{5}$$

where λ denotes the path loss exponent, d_0 denotes the reference distance, and d_1 is the distance between Alice and relay.

Therefore, the PDF and the cumulative distribution function (CDF) of $|h_{\mathrm{SR}}|^2$can be written as

$$f_{|h_{\mathrm{SR}}|^2}(y) = \frac{1}{G_{\mathrm{R}}} \left(\frac{y}{G_{\mathrm{R}}}\right)^{m_{\mathrm{R}}-1} \frac{1}{\Gamma(m_{\mathrm{R}})} {m_{\mathrm{R}}}^{m_{\mathrm{R}}} \exp\left(-m_{\mathrm{R}} \cdot \frac{y}{G_{\mathrm{R}}}\right), y \geq 0 \tag{6}$$

$$F_{|h_{\mathrm{SR}}|^2}(\mathrm{y}) = \frac{1}{\Gamma(m_{\mathrm{R}})} \gamma\left(m_{\mathrm{R}}, \frac{m_{\mathrm{R}} y}{G_{\mathrm{R}}}\right), y \geq 0 \tag{7}$$

where $\gamma(\cdot,\cdot)$ is the lower incomplete Gamma function [16, Eq. (8.350.1)].

2.2 VLC Link

In the indoor VLC network, it is assumed that the receiving area $\mathcal{P}$ is a disk with a radius$D$. As displayed in Fig. 1, Alice is projected at the center of the disk. In addition, we assume that Bob and Eve are deployed on the $\mathcal{P}$and subject to the uniform distribution. According to these, the PDF of Bob's (or Eve's) position is given by

$$f_U(u) = \frac{1}{\pi D^2}, u \in \mathcal{P} \tag{8}$$

$$f_W(w) = \frac{1}{\pi D^2}, w \in \mathcal{P} \tag{9}$$

where Urepresents the position of Bob and W represents the position of Eve.

The signals received by Bob or Eve in VLC link can be written as

$$Y_k = H_k X + Z_k, k = \text{BforBob}, k = \text{BforEve} \tag{10}$$

where $Z_k \sim N(0, \sigma_k^2)$ is the AWGN at Bob (or Eve) and σ_k^2 is the represents the variance of the corresponding noise.
The information is regarded as an instantaneous light intensity signal, so$X$must be non-negative [17]

$$X \geq 0 \tag{11}$$

The dimmable average optical intensity constraint is given by [17]

$$E(X) = \xi P, 0 \leq \xi \leq 1 \tag{12}$$

For general considerations, we assume that both Bob and Eve can receive the light from the LED. Therefore, the channel gain H_k of the VLC link could expressed as

$$H_k = \begin{cases} \frac{(m+1)A}{2\pi {d_k}^2} T_S g \cos^m(\phi_k) \cos(\psi_k), & 0 < \psi_k < \Psi_c \\ 0, & otherwise \end{cases} \tag{13}$$

where d_k represents the distance and irradiance angle between LED and Bob (or Eve) and ϕ_k is the radiation angle between them, A is the photodiode's physical area, m denotes the order of the Lambertian emission, g is the PD's concentrator gain, and T_S represents optical filter gain. Also, assuming that the normal vector between the receiving plane and the ceiling is vertical, we can obtain$\cos(\phi_k) = \cos(\varphi_k) = l/k$, where l represents perpendicular distance between the LED and the receiving plane [18]. Further, the H_k in (13) can be further expressed as

$$H_k = \frac{(m+1) A T_S g l^{m+1}}{2\pi} \left({r_k}^2 + l^2 \right)^{-\frac{m+3}{2}} \tag{14}$$

where r_k is the distance between the projection point O and Bob (or Eve).
According to (8) and (9): the CDF and the PDF of $r_k$can be expressed as

$$F_{r_k}(r_k) = \int_0^{2\pi} \int_0^{r_k} \frac{1}{\pi D^2} r dr d\theta = \frac{{r_k}^2}{D^2}, 0 < r_k \leq D \tag{15}$$

$$f_{r_k}(r_k) = \frac{dF_{r_k}(r_k)}{dr_k} = \frac{2r_k}{D^2}, 0 \leq r_k \leq D \tag{16}$$

where $\frac{dF_{r_k}(r_k)}{dr_k}$is the derivative of $dF_{r_k}(r_k)$with respect to r_k.

$$f_{H_k}(h) = \left| \frac{d}{dh} r_k \right| f_{r_k}(r_k) \tag{17}$$

Substituting (15) and (16) into (17): we can obtain the PDF of $H_k$as

$$f_{H_k}(h) = \Xi h^{-\frac{2}{m+3}-1}, \upsilon_{\min} \leq h \leq \upsilon_{\max} \tag{18}$$

where Ξ, $\upsilon_{\min}$ and$\upsilon_{\max}$ are

$$\Xi = \frac{2}{(m+3) D^2} \left(\frac{(m+1) A T_s g l^{m+1}}{2\pi} \right)^{\frac{2}{m+3}} \tag{19}$$

$$\upsilon_{\min} = \frac{(m+1) A T_s g l^{m+1}}{2\pi} \left(D^2 + l^2 \right)^{-\frac{m+3}{2}} \tag{20}$$

$$\upsilon_{\max} = \frac{(m+1) A T_s g l^{m+1}}{2\pi} l^{-(m+3)} \tag{21}$$

3 SOP ANALYSIS

In this subsection, the SOP performance of the hybrid system is analyzed. The instantaneous secrecy capacity (SC) of the first hop is its instantaneous channel capacity, i.e.,

$$C_{\text{hop},1} = \frac{1}{2} \log_2(1 + \gamma_{SR}) = \frac{1}{2} \log_2 \left(1 + \frac{P_s}{N_0} |h_{SR}|^2 \right) \tag{22}$$

Because the Shannon's capacity is not applicable to the VLC link [19]. Since there are constraints (11) and (12): the lower bound of the instantaneous SC is [20]

$$\begin{aligned} C_{\text{hop},2} &= \tfrac{1}{2} \log_2 \left(\frac{{\sigma_E}^2}{2\pi {\sigma_B}^2} \cdot \frac{e\xi^2 P^2 {H_B}^2 + 2\pi {\sigma_B}^2}{{H_E}^2 \xi^2 P^2 + {\sigma_B}^2} \right) \\ &= \tfrac{1}{2} \log_2 \left(\frac{1+J_B}{1+J_E} \right) \end{aligned} \tag{23}$$

Furthermore, the PDFs of $J_B$and J_E can be written as [14]

$$\begin{cases} f_{J_B}(j) = \frac{\Xi}{2} \left(\frac{2\pi\sigma_B^2}{e\xi^2 P^2} \right)^{-\frac{1}{m+3}} j^{-\frac{1}{m+3}-1} & J_{B,\min} \leq j \leq J_{B,\max} \\ f_{J_E}(j) = \frac{\Xi}{2} \left(\frac{\sigma_E^2}{\xi^2 P^2} \right)^{-\frac{1}{m+3}} j^{-\frac{1}{m+3}-1} & J_{E,\min} \leq j \leq J_{E,\max} \end{cases} \tag{24}$$

where $J_{B,\min} = \frac{e\xi^2 P^2 \upsilon_{\min}^2}{2\pi\sigma_B^2}$ and $J_{B,\max} = \frac{e\xi^2 P^2 \upsilon_{\max}^2}{2\pi\sigma_B^2}$, similarly $J_{E,\min} = \frac{\xi^2 P^2 \upsilon_{\min}^2}{\sigma_E^2}$ and $J_{E,\max} = \frac{\xi^2 P^2 \upsilon_{\max}^2}{\sigma_E^2}$.
As we all know, since the hybrid network can be seen as a series system, the capacity of this system depends on weakest channel [21]. So, the instantaneous SC of the entire hybrid system is the minimum of $C_{\text{hop},1}$ and $C_{\text{hop},2}$, which can be expressed as

$$C_I = \min \left(C_{\text{hop},1}, C_{\text{hop},2} \right) \tag{25}$$

The SOP is a significant performance metric to assess the PLS of a wireless communication network. The SOP can be written as

$$P_{SOP} = \Pr\{C_I < C_{th}\} \tag{26}$$

Substituting (25) into (26): the SOP is rewritten as

$$\begin{aligned} P_{SOP} &= \Pr\left\{ \min\left(C_{\text{hop},1}, C_{\text{hop},2} \right) < C_{th} \right\} \\ &= 1 - \Pr\left\{ \min\left(C_{\text{hop},1}, C_{\text{hop},2} \right) \geqslant C_{th} \right\} \\ &= 1 - \Pr\left\{ C_{\text{hop},1} \geqslant C_{th} \right\} \Pr\left\{ C_{\text{hop},2} \geqslant C_{th} \right\} \end{aligned} \tag{27}$$

where $C_{th} = \frac{1}{2} \ln(\gamma_{th})$ denotes the threshold of the targeted SC, γ_{th} represents the SNR's equivalent threshold [14]. It is worth be noted that obtaining the closed-form expression of $\Pr\{C_{\text{hop},2} \geq C_{th}\}$ is challenging, we assume that $\gamma_{th} \gg 1$. Alternatively, an upper bound of $\Pr\{C_{\text{hop},2} \geq C_{th}\}$ is given by

$$\Pr\left\{ C_{\text{hop},2} \geq C_{th} \right\} \leq 1 - \Pr\{J_B < J_E \gamma_{th}\} \tag{28}$$

Therefore, the lower-bounded of SOP is

$$\begin{aligned} P_{SOP} &= 1 - \left(1 - F_{|h_{SR}|^2} \left(\frac{(\gamma_{th}-1)N_0}{P_s} \right) \right) (1 - \Pr\{J_B < J_E \gamma_{th}\}) \\ &\triangleq P_{SOP_L} \end{aligned} \tag{29}$$

Based on these, the SOP's lower-bounded is further derived, as shown at the next page.

Table 1: Main parameters

	Parameters	Symbols	Values
RF	Reference distance	d_0	1Km
	Noise variance	N_0	1
	Transmission power at Alice	P_s	60dB
	Physical filter gain of PD	A	1cm^2
	PD's Optical filter gain	T_S	1
	PD's concentrator gain	g	3
VLC	Vertical distance between LED and floor	l	4m
	Order of Lambertian emission	m	2

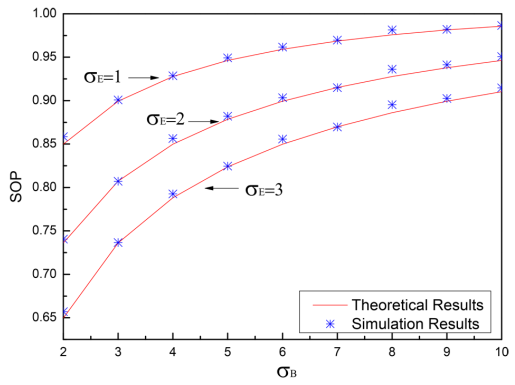

Figure 2: SOP performance versus Bob's noise standard deviation σ_B under different Eve's noise standard deviation σ_E when P=60dB,ξ =0.2, and γ_{th} =3.

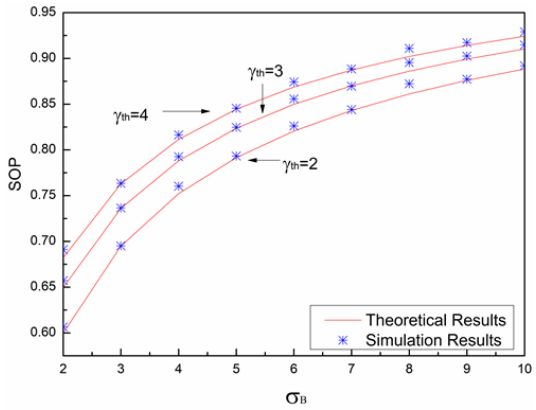

Figure 3: SOP performance versus Bob's noise standard deviation σ_B under different γ_{th} when P =60dB,ξ =0.2, σ_E=3.

4 NUMERICAL RESULTS

In this section, we will introduce the numerical results of hybrid RF/VLC systems. Here, the lower bound theoretical result of the derived SOP is verified by Monte-Carlo simulation, and the simulation result is executed by generating 10^4 random samples. Unless otherwise specified the main simulation parameters of the hybrid system are listed in TABLE 1.

Fig. 2 plots the SOP versus the Bob's noise standard deviationσ_B with different Eve's noise standard deviation $\sigma_E$when P=60 dB, ξ = 0.2, and γ_{th}=3. It can be noticed that as σ_B increase, the SOP performance becomes worse, because the larger σ_B is, the smaller channel gain $H_B$is. A larger H_B will lead to better secrecy performance, and a smaller H_B will degrade the secrecy performance. Besides, with σ_E increases, the secrecy performance also becomes better therefore by increasing of σ_E, H_E is reduced and smaller H_E leads to higher secrecy.

Fig. 3 plots SOP versus the Bob's noise standard deviation σ_B under different $\gamma_{th}$when P= 60 dB, ξ= 0.2, and σ_E = 3. As it is seen, the SOP increases with the $\sigma_B$increases, which is consistent with that in Figs. 2. Moreover, it can be noticed, with the increase of $\gamma_{th}$the secrecy performance of the system becomes worse.

Fig. 2 and Fig. 3 show that the simulation results are in good agreement with the theoretical results, which validates that our theoretical analysis of SOP is correct.

5 CONCLUSION

When VLC link is eavesdropped, the PLS performance of a hybrid RF/VLC DF-based relaying system is analyzed and the closed-form expression of the lower bound of SOP is obtained in this letter. It can be seen from the figure that the theoretical results agree well with the simulation results. Furthermore, when the VLC link is eavesdropped, the increase of the Bob's noise standard deviation and equivalent threshold of the SNR degrades the system secrecy performance, while the increase of Eve's noise standard deviation and floor radius will improve the secrecy performance.

ACKNOWLEDGMENTS

This work is supported by the National Nature Science Foundation of China (61701254, 11604133): the open fund of the Shandong Key Laboratory of Optical Communication Science and Technology in Liaocheng University (SDOC201901).

REFERENCES

[1] H. Tabassum and E. Hossain. 2018. Coverage and rate analysis for co-existing RF/VLC downlink cellular networks. *IEEE T. Wirel. Commun*, 17(4):2588-2601.
[2] T. Rakia, H. Yang, F. Gebali and M. Alouini. 2016. Optimal design of dual-hop VLC/RF communication system with energy harvesting. *IEEE Commun. Lett*, 20(10): 1979-1982.
[3}] M. Kashef, M. Ismail, M. Abdallah, K. A. Qaraqe and E. Serpedin. 2016. Energy efficient resource allocation for mixed RF/VLC heterogeneous wireless networks. *IEEE J. Sel. Area. Comm*, 34(4): 883-893.

$$P_{\mathrm{SOP_L}} = \begin{cases} \frac{P_{\mathrm{R}}}{\Gamma(m_{\mathrm{R}})}\gamma\left(m_{\mathrm{R}}, \frac{m_{\mathrm{R}}}{P_{\mathrm{R}}}\left(\frac{(\gamma_{\mathrm{th}}-1)N_0}{P_{\mathrm{S}}}\right)\right), & \text{if}\gamma_{\mathrm{th}} \le \frac{J_{\mathrm{B,min}}}{J_{\mathrm{E,max}}} \\ 1 - \frac{P_{\mathrm{R}}}{\Gamma(m_{\mathrm{R}})}\gamma\left(m_{\mathrm{R}}, \frac{m_{\mathrm{R}}}{P_{\mathrm{R}}}\left(\frac{(\gamma_{\mathrm{th}}-1)N_0}{P_{\mathrm{S}}}\right)\right) + \frac{P_{\mathrm{R}}}{\Gamma(m_{\mathrm{R}})}\gamma\left(m_{\mathrm{R}}, \frac{m_{\mathrm{R}}}{P_{\mathrm{R}}}\left(\frac{(\gamma_{\mathrm{th}}-1)N_0}{P_{\mathrm{S}}}\right)\right) \\ \times \varepsilon(m+3)^2 J_{\mathrm{B,min}}^{-\frac{1}{m+3}}\left[\left(\frac{J_{\mathrm{B,min}}}{\gamma_{\mathrm{th}}}\right)^{-\frac{1}{m+3}} - J_{\mathrm{E,max}}^{-\frac{1}{m+3}}\right] - \frac{\varepsilon}{2}(m+3)^2\gamma_{\mathrm{th}}^{-\frac{1}{m+3}}\left[\left(\frac{J_{\mathrm{B,min}}}{\gamma_{\mathrm{th}}}\right)^{-\frac{2}{m+3}} - J_{\mathrm{E,max}}^{-\frac{2}{m+3}}\right], & \text{if}\frac{J_{\mathrm{B,min}}}{J_{\mathrm{E,max}}} < \gamma_{\mathrm{th}} \le \frac{J_{\mathrm{B,min}}}{J_{\mathrm{E,min}}} \\ 1 - \frac{P_{\mathrm{R}}}{\Gamma(m_{\mathrm{R}})}\gamma\left(m_{\mathrm{R}}, \frac{m_{\mathrm{R}}}{P_{\mathrm{R}}}\left(\frac{(\gamma_{\mathrm{th}}-1)N_0}{P_{\mathrm{S}}}\right)\right) + \frac{P_{\mathrm{R}}}{\Gamma(m_{\mathrm{R}})}\gamma\left(m_{\mathrm{R}}, \frac{m_{\mathrm{R}}}{P_{\mathrm{R}}}\left(\frac{(\gamma_{\mathrm{th}}-1)N_0}{P_s}\right)\right) \\ \times \varepsilon(m+3)^2 J_{\mathrm{B,min}}^{-\frac{1}{m+3}}\left[J_{\mathrm{E,min}}^{-\frac{1}{m+3}} - \left(\frac{J_{\mathrm{B,max}}}{\gamma_{\mathrm{th}}}\right)^{-\frac{1}{m+3}}\right] - \frac{\varepsilon}{2}(m+3)^2\gamma_{\mathrm{th}}^{-\frac{1}{m+3}}\left[J_{\mathrm{E,min}}^{-\frac{2}{m+3}} - \left(\frac{J_{\mathrm{B,max}}}{\gamma_{\mathrm{th}}}\right)^{-\frac{2}{m+3}}\right] & \text{if}\frac{J_{\mathrm{B,min}}}{J_{\mathrm{E,min}}} < \gamma_{\mathrm{th}} < \frac{J_{\mathrm{B,max}}}{J_{\mathrm{E,min}}} \\ + \varepsilon(m+3)^2\left(J_{\mathrm{B,min}}^{-\frac{1}{m+3}} - J_{\mathrm{B,max}}^{-\frac{1}{m+3}}\right) \times \left[\left(\frac{J_{\mathrm{B,max}}}{\gamma_{\mathrm{th}}}\right)^{-\frac{1}{m+3}} - J_{\mathrm{E,max}}^{-\frac{1}{m+3}}\right], & \\ 1, & \text{if}\gamma_{\mathrm{th}} \ge \frac{J_{\mathrm{B,max}}}{J_{\mathrm{E,min}}} \end{cases} \tag{30}$$

[4] M. Hammouda, S. Akin, A. M. Vegni, H. Haas and J. Peissig. 2018. Link selection in hybrid RF/VLC systems under statistical queueing constraints. *IEEE T. Wirel. Commun*, 17(4): 2738-2754.

[5] J. Kong, M. Ismail, E. Serpedin and K. A. Qaraqe. 2019. Energy efficient optimization of base station intensities for hybrid RF/VLC networks. *IEEE T. Wirel. Commun*, 18 (8): 4171-4183.

[6] Y. Hsiao, Y. Wu and C. Lin. 2019. Energy-efficient beamforming design for MU-MISO mixed RF/VLC heterogeneous wireless networks. *IEEE T. Signal Proces*, 67(14): 3770-3784.

[7] M. F. Marzban, M. Kashef, M. Abdallah and M. Khairy. 2017. Beamforming and power allocation for physical-layer security in hybrid RF/VLC wireless networks. *In 2017 13th International Wireless Communications and Mobile Computing Conference (IWCMC)*: 258-263.

[8] T. Rakia, H. C. Yang, F. Gebali and M. S. Alouini. 2016. Dual-hop VLC/RF transmission system with energy harvesting relay under delay constraint. *In 2016 IEEE Globecom Workshops (GC Wkshps)*:1-6.

[9] H. Abuella, M. Elamassie, M.Uysal , Z. Xu , E and Serpedin, K. A. 2007.Qaraqe, and S. Ekin, Hybrid RF/VLC Systems: A Comprehensive Survey on Network Topologies, Performance Analyses, Applications, and Future Directions. *arXiv preprint arXiv*,02466.

[10] P. C. Pinto, J. Barros and M. Z. Win. 2011. Secure communication in stochastic wireless networks part II: Connectivity. *IEEE T. INF. FOREN. SEC*, 7(1):125-138.

[11] J. Zhang, T. Q. Duong, R. Woods and A. Marshall. 2017. Securing wireless communications of the Internet of things from the physical layer, an overview. *Entropy,* 19(8): 420.

[12] J. Al-Khori, G. Nauryzbayev, M. M. Abdallah and M. Hamdi. 2019. Secrecy performance of decode-and-forward based hybrid RF/VLC relaying systems. *IEEE Access*, 7, 10844-10856.

[13] A. Kumar, P. Garg and A. Gupta.2020. PLS analysis in an indoor heterogeneous VLC/RF network based on known and unknown CSI. *IEEE Syst. J.*, DOI: 10.

[14] J. Y. Wang, Y. Qiu, S. H. Lin, J. B. Wang, Q. Wang and B. Zhang. 2020. Performance analysis and improvement for secure VLC with SLIPT and random terminals. *IEEE Access*, 8, 73645-73658.

[15] M. K. Simon and M. S. Alouini. 2005. *Digital communication over fading channels* (2nd. ed.): Wiley.

[16] I. S. Gradshteyn and I. M. Ryzhik. 2007. Table of integrals, series, and products. *Elsevier Academic Press.*

[17] J. B. Wang, Q. S. Hu, J. Wang, M. Chen and J. Y. Wang. 2013. Tight bounds on channel capacity for dimmable visible light communications. *J. Lightwave Technol*, 31(23): 3771-3779.

[18] T. Komine and M. Nakagawa. 2004. Fundamental analysis for visible-light communication system using LED lights. *IEEE T. Consum. Electr.*50(1):100-107.

[19] L. Yin and H. Haas. 2018. Physical-layer security in multiuser visible light communication networks. *IEEE J. Sel. Area. Comm*, 36(1):162-174.

[20] J. Y. Wang, C. Liu, J. B. Wang, Y. Wu, M. Lin and J. Cheng. 2018. Physical layer security for indoor visible light communications: Secrecy capacity analysis. *IEEE T. Commun*, *66(*12): 6423-6436.

[21] Y. Ai, A. Mathur, M. Cheffena, M. R. Bhatnagar and H. Lei.2019. Physical-layer security of hybrid satellite-FSO cooperative systems. *IEEE Photonics J.*, 11(1): 1-14.